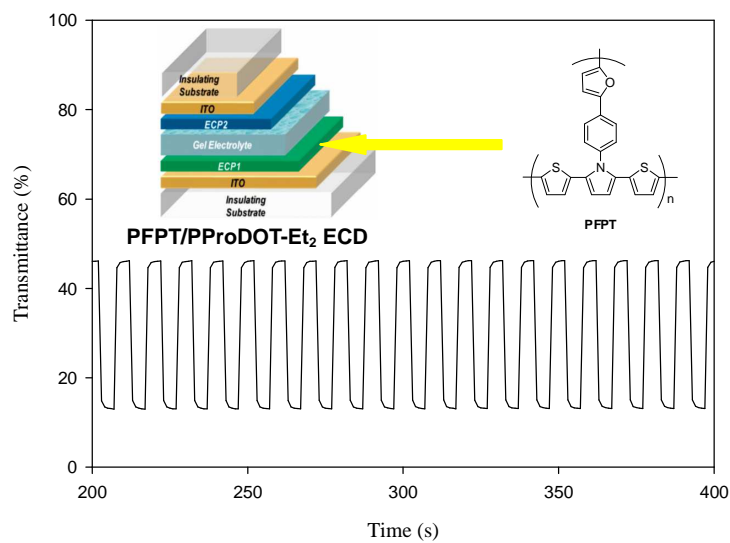


Graphical Abstract



A PFPT/PProDOT-Et₂ ECD attained a high ΔT (33.3% at 590 nm) and a high η (533.5 cm² C⁻¹ at 590 nm).

4-(Furan-2-yl)phenyl-containing polydithienylpyrroles as promising electrodes for high contrast and coloration efficiency electrochromic devices

Wen-Hsin Wang^a, Jui-Cheng Chang^b, Tzi-Yi Wu^{a,*}

^a Department of Chemical and Materials Engineering, National Yunlin University of Science and Technology, Yunlin 64002, Taiwan, ROC

^b Bachelor Program in Interdisciplinary Studies, National Yunlin University of Science and Technology, Yunlin 64002, Taiwan, ROC

* Correspondence: wuty@yuntech.edu.tw.

ABSTRACT

A 4-(furan-2-yl)phenyl-containing conjugated dithienylpyrrole (FPT) was prepared using a Paal-Knorr reaction and its homologous homopolymer (PFPT) and copolymers (P(FPT-co-DTC) and P(FPT-co-DTP)) were electrosynthesized. Spectroelectrochemical investigations displayed that PFPT film was saffron yellow (0 V) in a reduced state, yellowish-gray (1.0 V), light purple (1.2 V), and bluish-purple (1.4 V) in an oxidized state. P(FPT-co-DTC) film was green, grayish-green, grayish-blue, and bluish-purple from reduced to oxidized states. Electrochromic switching studies revealed the transmittance change (ΔT) of PFPT, P(FPT-co-DTC), and P(FPT-co-DTP) films were 22.7%, 44.8%, and 50.7% at 1320 nm, 906 nm, and 1212 nm, respectively, and the coloration efficiency (η) of PFPT, P(FPT-co-DTC), and P(FPT-co-DTP) films were estimated to be 181.8 cm² C⁻¹, 229.0 cm² C⁻¹, and 232.4 cm² C⁻¹ at 1320 nm, 906 nm, and 1212 nm, respectively. A P(FPT-co-DTP)/PProDOT-Et₂ ECD revealed a high ΔT (38.6% at 612 nm) and rapid switching time, whereas a PFPT/PProDOT-Et₂ ECD attained a high ΔT (33.3% at 590 nm), a high η (533.5 cm² C⁻¹ at 590 nm) and long-term reversible redox behaviors.

Keywords: 4-(furan-2-yl)phenyl, spectroelectrochemistry, electrochromic switching, electrochromic device, long-term cycling stability

1. Introduction

Electrochromic materials have taken an interest in academic scientists due to their promising applications as electrochromic car window film, auto-dimming rear-view mirror and light adjusting sunglasses [1]. In the past two decades, both organic materials (diphthalocyanine, viologen, tetrathiafulvalene, and conjugated polymer) and inorganic materials (WO_3 , V_2O_5 , NiO , IrO_2 , and MoO_3) materials have been developed to be used in electrochromic devices. Although inorganic electrochromic materials present considerable benefits regarding their high optical contrast and electrical durability, organic electrochromic materials show some benefits over inorganic electrochromic materials due to their fast electrochromic switching, high coloration efficiency, ease of processing and multicolor electrochromism, etc [2]. Recently, interest has focused on the research of conjugated polymers as organic electrochromic materials in ECDs [3]. Polythiophene [4,5], polyimides [6,7], polyindoles [8], polycarbazole [9-12], poly(3,4-ethylenedioxythiophene) (PEDOT) [13], poly(3,4-propylenedioxythiophene) (PProDOT) [14], polytriphenylamine [15,16], and polyaniline [17] have been applied widely in various organic electrochromic devices. Among these conjugated polymers, polythiophenes have been extensively studied due to their good redox reversibility, attractive optoelectronic properties and high electrical and environmental stability. PEDOT and PProDOT are common derivatives of polythiophenes, which comprise two electron-donating atoms on 3,4-positions of polythiophenes. PEDOT and PProDOT show lower onset oxidation potentials than those of polythiophenes [18]. Moreover, important optoelectronic properties of PEDOT and PProDOT are low transmissivity at their reduced state and high transmissivity at their oxidized state, which are known as reduced state blue organic electrochromic materials [19]. Polydithienylpyrroles (PSNS) and their derivatives are also most promising polythiophenes derivatives, the onset oxidation potentials (0.7 V vs.

Ag/AgCl [20]) of PSNS derivatives are less than those of polythiophenes, PEDOT, and PProDOT. Low onset oxidation potential leads PSNS derivatives to have high-lying HOMOs and can be oxidized facily during redox processes. Ak et al. reported the synthesis and electrochromic characterization of a dithienylpyrrole based copolymer (P(TPVB-*co*-EDOT)), the copolymer revealed high transmittance change (75% at 1000 nm), satisfactory switching response, and reasonable stability [21]. Ozkut and Cihaner et al. synthesized a conjugated copolymer (P(EDOT-*co*-1)) using electropolymerization, P(EDOT-*co*-1) revealed five color variations ranging from dark purple, purple, gray, green to cyan. Moreover, P(EDOT-*co*-1) displayed a high ΔT (41%), a high η (258 cm² C⁻¹), and fast switching time (1.4 s) [22]. On the other hand, furan is a donor unit, the incorporation of furan unit in polymer backbone is beneficial for enhancing the hole transporting ability of polymer. 3,6-di(2-thienyl)carbazole (DTC) and dithieno[3,2-b:2',3'-d]pyrrole (DTP) units reveal similar structures to dithienylpyrroles. However, DTP unit presents a fused-ring thiophene and a conjugated planar ring structures, which enhances effective conjugation length and red-shifts the UV-vis absorption spectra [23].

So far, the incorporation of a 4-(furan-2-yl)phenyl group into the pyrrole unit of dithienylpyrrole and the investigation of electrochromic behaviors of its corresponding polymer films have not been carried out yet. In the present work, 4-(furan-2-yl)phenyl-containing PFPT, P(FPT-*co*-DTC), and P(FPT-*co*-DTP) films are employed as the anodically coloring materials in dual type ECDs, and a poly(3,4-(2,2-diethylpropylenedioxy)thiophene) (PProDOT-Et₂) film is employed as the cathodically coloring material in dual type ECDs. The electrochromic behaviors and color-bleach kinetics of PFPT, P(FPT-*co*-DTC), and P(FPT-*co*-DTP) films and spectroelectrochemistry, redox stabilities, and optical memory of their corresponding ECDs are investigated exhaustively.

2. Experimental

2.1. Materials

Furan, 4-nitroaniline, isoamyl nitrite, and other starting chemicals were purchased from Aldrich, Acros, Tokyo Chemical Industry (TCI), Merck, and used as received. The monomer (ProDOT-Et₂) of cathodic layer and 1-ethyl-3-propylimidazolium bis(trifluoromethanesulfonyl)imide ([EPI⁺][TFSI⁻]) were prepared in accordance with previously published methods [24-26]. Anodic polymer films were either prepared potentiodynamically with a potential range of -1.0 V to 1.8 V or potentiostatically at 0.9 V on conductive glasses. The reference electrode used in the preparation of polymer films is an Ag/AgCl electrode. P(FPT-co-DTC) and P(FPT-co-DTP) films were coated using a feed molar ratio of either FPT/DTC or FPT/DTP at 1/1. The length and width of electrochromic electrodes are 1.5 and 1 cm, respectively.

2.2. Synthesis of 2-(4-nitrophenyl)furan (Scheme 1)

A 100 mL round-bottomed flask equipped with a magnetic mixer was charged with furan (2.04 g, 30 mmol), 4-nitroaniline (2.76 g, 20 mmol), isoamyl nitrite (3.51 g, 30 mmol), and 120 mL acetonitrile (ACN). The solution was stirred for 7 h at 25 °C. After evaporating off ACN, the remaining product was purified using a column chromatography on silica with an eluent (dichloromethane/hexane = 1/4). Yield: 61%. ¹H NMR (700 MHz, DMSO-*d*₆): δ 8.27 (d, 2H, phenyl-H), 7.95 (d, 3H, phenyl-H and Fu-H), 7.32 (d, 1H, Fu-H), 6.71 (dd, 1H, Fu-H). ¹³C NMR (125 MHz, DMSO-*d*₆): δ 110.4, 113.0, 124.1, 124.5, 136.1, 145.4, 146.0, 151.1. Elem. anal. calcd. for C₁₀H₇NO₃: C, 63.49%; H, 3.73%; N, 7.40%. Found: C, 63.31%; H, 3.66%; N, 7.28%.

2.3. Synthesis of 4-(furan-2-yl)aniline

A 100 mL round-bottomed flask equipped with a magnetic mixer was charged with

2-(4-nitrophenyl)furan (0.95 g, 5 mmol), $\text{NH}_2\text{NH}_2 \cdot \text{H}_2\text{O}$ (0.15 g, 3 mmol), 5 mg Pd/C, and 15 mL EtOH, and the solution was stirred for a day under reflux. After evaporating off EtOH under reduced pressure, the remaining product was purified using a column chromatography on silica with an eluent (dichloromethane/hexane = 1/1). Yield: 74 %. ^1H NMR (700 MHz, $\text{DMSO-}d_6$): δ 7.56 (d, 1H, Fu-H), 7.35 (d, 2H, phenyl-H), 6.58 (d, 2H, phenyl-H), 6.53 (d, 1H, Fu-H), 6.47 (dd, 1H, Fu-H), 5.29 (s, 2H, phenyl-NH₂-). ^{13}C NMR (125 MHz, $\text{DMSO-}d_6$): δ 101.8, 111.8, 114.1, 118.8, 124.8, 140.9, 148.5, 154.6. Elem. anal. calcd. for $\text{C}_{10}\text{H}_9\text{NO}$: C, 75.45 %; H, 5.70 %; N, 8.80 %. Found: C, 75.27%; H, 5.63%; N, 8.71%.

2.4. Synthesis of 1-(4-(furan-2-yl)phenyl)-2,5-di(thiophen-2-yl)pyrrole (FPT)

A 100 mL round-bottomed flask equipped with a magnetic mixer was charged with 1,4-di(2-thienyl)-1,4-butanedione (2.1 mmol, 0.53 g), 4-(furan-2-yl)aniline (6.3 mmol, 1 g), 22 mL toluene, and 12 mg *p*-TSA, and the solution was stirred for 18 h at 110 °C. After evaporating off toluene using a rotavapor, the remaining product was purified using a column chromatography on silica with an eluent (dichloromethane/hexane = 1/2). Yield: 63 %. ^1H -NMR (700 MHz, $\text{DMSO-}d_6$): δ 7.82 (d, 3H, Fu-H and phenyl-H), 7.39 (d, 2H, phenyl-H), 7.29 (d, 2H, Th-H), 7.11 (d, 1H, Fu-H), 6.88 (dd, 2H, Th-H), 6.72 (d, 2H, Th-H), 6.65 (dd, 1H, Fu-H), 6.58 (d, 2H, Py-H). ^{13}C NMR (125 MHz, $\text{DMSO-}d_6$): δ 107.4, 109.7, 112.4, 124.2, 124.4, 125.0, 127.2, 129.8, 130.7, 131.3, 134.0, 136.6, 143.7, 152.0. Elem. anal. calcd. for $\text{C}_{22}\text{H}_{15}\text{NOS}_2$: C, 70.75%; H, 4.05%; N, 3.75%. Found: C, 70.58%; H, 3.97%; N, 3.62%.

2.5. Fabrication of ECDs

Dual type PFPT/PProDOT-Et₂, P(FPT-*co*-DTC)/PProDOT-Et₂, and P(FPT-*co*-DTP)/PProDOT-Et₂ ECDs were fabricated by sandwiching the electrolyte

layer between two complementary polymer films. The anodic polymer layers were PFPT, P(FPT-*co*-DTC), and P(FPT-*co*-DTP) films, the cathodic polymer layer was a PProDOT-Et₂ film, and the electrolyte layer was an [EPI⁺][TFSI⁻]/PVdF-HFP composite electrolyte, which was prepared based on our previous works [26]. The anodic and cathodic coloring layers were coated on indium tin oxide (ITO) substrates at 0.9 and +1.4 V, respectively.

2.6. Spectroelectrochemical and electrochemical properties

Spectroelectrochemical characteristics of polymer films and ECDs were measured using a UV-Vis-NIR spectrophotometer (JASCO V-670) and an electrochemical analyzer (CHI660a). The electrochemical cell for electrochemical measurements includes an ITO glass as working electrode (WE), a platinum wire as counter electrode (CE), Ag/AgCl as reference electrode (RE), and the electrodes are immersed in 0.1 M LiClO₄/ACN electrolyte. The onset potential of oxidation was estimated using the first CV cycle.

3. Results and discussion

3.1. Electrochemical polymerization

Fig. 1 shows the cyclic voltammetric curves for the repeated scanning electropolymerization of FPT, DTC, and DTP monomers and their mixtures. As the voltammetric curves increased with increasing number of cycles, the PFPT, P(FPT-*co*-DTC), and P(FPT-*co*-DTP) films could be seen on the ITO transparent conductive glass, demonstrating the polymer films were coated on the ITO conductive substrate [27]. As presented in Fig. 1, the onset oxidation potential of FPT, DTC, and DTP were 0.74, 0.82, and 0.80 V, respectively. The onset oxidation potential disparity of these monomers is less than 0.1 V, implying the copolymerization of FPT

and DTC (or DTP) was feasible. Moreover, the onset oxidation potential of FPT was less than those of DTC and DTP, indicating that 4-(furan-2-yl)phenyl-containing dithienylpyrrole was easier to oxidize than either the DTC or DTP. Figs. 1(d) and 1(e) showed the cyclic voltammetric experiments using mixtures of two monomers ((FPT + DTC) and (FPT + DTP)) in solutions. Obviously, the oxidation peaks, reduction peaks, and cyclic voltammetric wave-shapes of P(FPT-co-DTC) and P(FPT-co-DTP) films were different to those of PFPT, PDTC, and PDTP films, which indicated copolymer films were electrodeposited on ITO substrates. The schemes of coelectropolymerization were displayed in Scheme 2.

The PFPT film was scanned in monomer-free 0.1 M LiClO₄/ACN solution at different sweep rates. As shown in Fig. 2, PFPT film exhibited well-defined redox processes. A linear increase in the anodic and cathodic currents as a function of the scanning rates indicated that the electroactive species migrated during the redox process were non-diffusional controlled and PFPT film was bounded to the ITO electrode tightly [28].

3.2. Spectral analysis of polymer films

Fig. 3 showed the UV-visible-NIR spectra of PFPT, P(FPT-co-DTC), and P(FPT-co-DTP) films at various potentials. PFPT film revealed an absorption shoulder at 407 nm, which could be ascribed to the π - π^* transition of PFPT film. When the applied voltages increased gradually, the absorbance of π - π^* transition bands weakened gradually and polaron and bipolaron bands emerged and heightened at around 590 and 1320 nm [29]. P(FPT-co-DTC) film shows similar π - π^* transition shoulder at 406 nm, the polaron and bipolaron peaks shift to 906 nm. However, the π - π^* transition absorption band of P(FPT-co-DTP) film shifted bathochromically to 472 nm in [EPI⁺][TFSI⁻] solution, implying the dithieno[3,2-b:2',3'-d]pyrrole unit of

P(FPT-*co*-DTP) backbone displayed satisfactory π -conjugation across fused thiophene rings [30]. The polaron (or bipolaron) band of P(FPT-*co*-DTP) film shifted bathochromically to 1212 nm.

Table 1 revealed the electrochromic images and L^* , a^* , b^* values of PFPT, P(FPT-*co*-DTC), and P(FPT-*co*-DTP) films at various potentials in [EPI⁺][TFSI] solution. PFPT film was saffron yellow (0 V) in a reduced state, yellowish-gray (1.0 V), light purple (1.2 V), and bluish-purple (1.4 V) in an oxidized state. P(FPT-*co*-DTC) and P(FPT-*co*-DTP) films displayed four color variations from reduced to oxidized states. P(FPT-*co*-DTC) film was green, grayish-green, grayish-blue, and bluish-purple at 0, 1.0, 1.2, and 1.4 V, respectively. P(FPT-*co*-DTP) film was brass, gray, grayish-blue, and blue at 0, 0.8, 1.0, and 1.2 V, respectively. The CIE chromaticity charts of PFPT, P(FPT-*co*-DTC), and P(FPT-*co*-DTP) films in an ionic liquid solution in reduced and oxidized states are shown in Fig. S1 (in supplementary information).

The optical band gap (E_g) of PFPT film calculated using the onset wavelength of the π - π^* transition peak was 2.26 eV [31]. Table 2 summarizes the comparison of E_g with reported polymer films, PFPT film shows comparable E_g to those reported for P(TPHA) [32] and PSNS-iProP [33]. However, the E_g of PFPT film is smaller than those reported for PSNS-Fc [34] and P(SNS-pyrene) [35], which can be ascribed to the incorporations of ferrocene and pyrene as the anchored group of PSNS derivatives increasing the E_g significantly. The oxidation onset potential of PFPT (vs. Ag/AgCl) was 0.74 V, the E_{FOC} value determined from ferrocene/ferrocenium (Fc/Fc⁺) (vs. Ag/AgCl) was 0.57 V, and the $E_{\text{onset(ox)}}$ (vs. E_{FOC}) was estimated as 0.17 V. The HOMO energy level of PFPT calculated from the $E_{\text{onset(ox)}}$ and the energy level of the Fc/Fc⁺ couple (4.8 eV below the vacuum level (zero eV)) [36,37] was taken as -4.97 eV. The LUMO energy level of PFPT relative to the vacuum level was estimated to be -2.71 eV.

3.3. Color-bleach kinetics of polymer films

The potentials of PFPT, P(FPT-*co*-DTC), and P(FPT-*co*-DTP) films were interchanged between 0 (the reduced state) and 1.0 V (the oxidized state) with a time interval of 5 s in a solution. The dynamic electrochromic switching profiles of the three films in an ionic liquid are displayed in Fig. 4, and their coloration and bleaching switching times (τ_c and τ_b) estimated at 90% of entire transmittance change and calculated at various cycles are listed in Table S1 (in supplementary information). The τ_c and τ_b of three polymer films at various cycles and wavelengths were estimated to be 1.71-2.46 s in an ionic liquid solution.

The transmittance variations between the reduced and oxidized states of the PFPT, P(FPT-*co*-DTC), and P(FPT-*co*-DTP) films were 22.7%, 44.8%, and 50.7% at 1320 nm, 906 nm, and 1212 nm, respectively, at the first cycle. The ΔT of P(FPT-*co*-DTC) and P(FPT-*co*-DTP) films in near-infrared region increased significantly compared to that of PFPT film in an ionic liquid solution, implying DTC- and DTP-containing copolymers displayed higher ΔT in the near-infrared zone than that of PFPT homopolymer. The transmittance variations for the PFPT, P(FPT-*co*-DTC), and P(FPT-*co*-DTP) films in the near-infrared zone are larger than those in UV-Vis zone, this can be attributed to the formation of significant charge carriers upon doping. Table 2 lists the comparison of transmittance change with the reported polymer films in electrolytes. PFPT film reveals a higher ΔT_{\max} than those reported for P(TPHA) at 334 nm [32], PSNS-iProP at 646 nm [33], and P(SNS-pyrene) at 349 nm [35]. However, the ΔT_{\max} of PFPT film is lower than that of PSNS-Fc at 356 nm [34].

The discrepancy of optical density (ΔOD) at specific wavelength can be calculated using the following formula,

$$\Delta OD = \log\left(\frac{T_{ox}}{T_{red}}\right), \quad (1)$$

where T_{ox} and T_{red} denote the transmittance at oxidized and reduced states, respectively.

As presented in Table 2, the PFPT film displayed higher ΔOD than that reported for PSNS-iProP at 646 nm [33].

Another crucial parameter of electrochromic polymer films is coloration efficiency (η), which can be determined from the following formula:

$$\eta = \frac{\Delta OD}{Q_d}, \quad (2)$$

where Q_d represents the injected/ejected electronic charge per unit electrode area. As shown in Table 2, the η_{max} of PFPT, P(FPT-co-DTC), and P(FPT-co-DTP) films in [EPI⁺][TFSI⁻] were estimated to be 181.8 cm² C⁻¹ at 1320 nm, 229.0 cm² C⁻¹ at 906 nm, and 232.4 cm² C⁻¹ at 1212 nm, respectively. Although PFPT displayed lower η_{max} than those of P(FPT-co-DTC) and P(FPT-co-DTP) films, PFPT film presented higher η than those reported for PSNS-iProP at 646 nm [33] and P(SNS-pyrene) at 349 nm [35].

3.4. Spectroelectrochemical behaviors of ECDs

Figs. 5(a), 5(b), and 5(c) exhibit the UV-Vis spectra of dual type PFPT/PProDOT-Et₂, P(FPT-co-DTC)/PProDOT-Et₂, and P(FPT-co-DTP)/PProDOT-Et₂ ECDs at several potentials. PFPT/PProDOT-Et₂, P(FPT-co-DTC)/PProDOT-Et₂, and P(FPT-co-DTP)/PProDOT-Et₂ ECDs presented precise absorption shoulders or peaks at ca. 407, 406, and 472 nm at 0 V, respectively, which were in agreement with the π - π^* transition of PFPT, P(FPT-co-DTC), and P(FPT-co-DTP) films in neutral states. In the circumstance, the PProDOT-Et₂ layer was classified as in an oxidized state and presented no conspicuous characteristic peak in the UV-Vis zone [38]. An increase of applied voltage resulted in the oxidation of

anodically coloring layers and the reduction of the cathodically coloring layers. Accordingly, absorption peaks of ECDs started to appear at 586-612 nm, the preeminent color of three ECDs was dark blue at a voltage $\geq +1.2$ V as displayed in Table 3. Fig. S2 (in supplementary information) exhibited the chromaticity diagrams of these dual type ECDs at -0.4 and 1.2 V.

3.5. Color-bleach kinetics of ECDs

As presented in Fig. 6, the color-bleach kinetics of PFPT/PProDOT-Et₂, P(FPT-co-DTC)/PProDOT-Et₂, and P(FPT-co-DTP)/PProDOT-Et₂ ECDs were interchanged between -0.2 (the bleached state) and +1.2 V (the colored state) with a time interval of 5 s. The τ_c and τ_b of these ECDs estimated at various cycles are summarized in Table 4, which were shorter than those of their corresponding polymer films in solutions. This can be ascribed to the ECDs showed short distance between working and counter electrodes [39]. Furthermore, the ΔT_{\max} of PFPT/PProDOT-Et₂, P(FPT-co-DTC)/PProDOT-Et₂, and P(FPT-co-DTP)/PProDOT-Et₂ ECDs as shown in Table 4 were 33.3, 29.9, and 37.5%, respectively, from -0.2 V (the bleached state) to +1.2 V (the colored state). Therefore, the ECD employing P(FPT-co-DTP) as an anodically coloring film displayed the highest ΔT_{\max} among the three ECDs.

As listed in Table 5, the η of ECDs were 533.5, 340.0, and 855.9 cm² C⁻¹ for PFPT/PProDOT-Et₂ ECD at 590 nm, P(FPT-co-DTC)/PProDOT-Et₂ ECD at 586 nm, and P(FPT-co-DTP)/PProDOT-Et₂ ECD at 612 nm, respectively. Hence, the ECD employing a P(FPT-co-DTP) anodically coloring film revealed the highest η , and a P(FPT-co-DTC) anodically coloring film displayed the lowest η among the three ECDs.

As shown in Table 5, the ΔT_{\max} and η of PFPT/PProDOT-Et₂, P(FPT-co-DTC)/PProDOT-Et₂, and P(FPT-co-DTP)/PProDOT-Et₂ ECDs were

compared with previous reported works. PFPT/PProDOT-Et₂ ECD displayed higher ΔT_{\max} than those reported for P(TPHA-co-EDOT)/PEDOT [32], PBTC/PEDOT [40], PBEC/PEDOT [40], and PBDO/PProDOT-Et₂ ECDs [41]. Moreover, PFPT/PProDOT-Et₂ ECD obtained a higher η than those reported for PBTC/PEDOT [40], PBEC/PEDOT [40], and PBDO/PProDOT-Et₂ ECDs [41].

3.6. Open-circuit memory of ECDs

The transmittance-time profiles of PFPT/PProDOT-Et₂, P(FPT-co-DTC)/PProDOT-Et₂, and P(FPT-co-DTP)/PProDOT-Et₂ ECDs in different electrochromic states were measured at 590, 586 and 612 nm, respectively. The applied potentials in bleached and colored states are 1 s during each 200 s time interval. As shown in Fig. 7, the transmittance changes were less than 3% in bleached (-0.2 V) and colored (+1.2 V) states of the three ECDs, revealing that these ECDs had adequate optical memory.

3.7. Electrochemical stability of ECDs

The electrochemical cycling stability of ECDs scanned between -1.0 V and +1.8 V is carried out using CV [42]. As displayed in Fig. 8, the electrochemical activity of PFPT/PProDOT-Et₂, P(FPT-co-DTC)/PProDOT-Et₂, and P(FPT-co-DTP)/PProDOT-Et₂ ECDs was 93.7%, 96.0%, and 94.1%, respectively, after scanning between -1.0 V and +1.8 V for 500 cycles. 90.9%, 95.6%, and 93.1% of electrochemical activity was maintained after 1000 cycles for PFPT/PProDOT-Et₂, P(FPT-co-DTC)/PProDOT-Et₂, and P(FPT-co-DTP)/PProDOT-Et₂ ECDs, respectively. The electrochemical activities of PFPT/PProDOT-Et₂, P(FPT-co-DTC)/PProDOT-Et₂, and P(FPT-co-DTP)/PProDOT-Et₂ ECDs at 500th cycle are larger than those reported for imidazole-containing polymer (P1)/PEDOT ECD (stability = 81.3% at 500th cycle)

[43] and PBTC/PEDOT ECD (stability = 92% at 500th cycle) [40]. The results indicate that the anodically coloring films are potential for using in ECDs.

4. Conclusions

Three 4-(furan-2-yl)phenyl-containing conjugated polydithienylpyrroles (PFPT, P(FPT-*co*-DTC), and P(FPT-*co*-DTP)) were electrosynthesized on conductive ITO glass using potentiodynamic and potentiostatic depositions. The polymer films displayed reversible redox behaviors and multichromic properties. P(FPT-*co*-DTP) film displayed conspicuous color variations ranging from brass, gray, grayish-blue to blue. Electrochromic switching studies of polymer films revealed that P(FPT-*co*-DTP) film attained a higher ΔT_{\max} (50.7%) and η_{\max} (232.4 cm² C⁻¹) at 1212 nm than those of PFPT and P(FPT-*co*-DTC) films. Moreover, three dual-type ECDs based on three anodically coloring materials and a cathodically coloring material were fabricated. PFPT/PProDOT-Et₂ ECD realized high ΔT_{\max} (33.3%), ΔOD_{\max} (53.4%) and η (533.5 cm² C⁻¹). In addition, PFPT/PProDOT-Et₂, P(FPT-*co*-DTC)/PProDOT-Et₂, and P(FPT-*co*-DTP)/PProDOT-Et₂ ECDs displayed short switching time (≤ 1.03 s) and long-term electrochemical cycling stability. Owing to the promising outcomes, the three anodically coloring materials are potential candidates as electrochromic layers for ECDs.

References

- [1] C.G. Granqvist, P.C. Lansåker, N.R. Mlyuka, G.A. Niklasson, E. Avendaño, *Solar Energy Mater. Solar Cells* 93 (2008) 2032.
- [2] E. Rustaml, S. Goker, S. Tarkuc, Y.A. Udum, L. Toppare, *J. Electrochem. Soc.* 162 (2015) G75.
- [3] S.-H. Hsiao, Y.-P. Huang, *Dyes Pigm.* 158 (2018) 368.
- [4] K. Lin, S. Zhang, H. Liu, Y. Zhao, Z. Wang, J. Xu, *Int. J. Electrochem. Sci.* 10 (2015) 7720.
- [5] B. Gadgil, P. Damlin, E. Dmitrieva, T. Ääritalo, C. Kvarnström, *RSC Adv.* 5 (2015) 42242.

- [6] S.-H. Hsiao, W.-K. Liao, G.-S. Liou, *Polymers* 9 (2017) 511.
- [7] S.-H. Hsiao, Y.-Z. Chen, *J. Electroanal. Chem.* 799 (2017) 417.
- [8] C.W. Kuo, T.Y. Wu, M.W. Huang, *J. Taiwan Inst. Chem. Eng.* 68 (2016) 481.
- [9] C.W. Kuo, P.Y. Lee, *Polymers* 9 (2017) 518.
- [10] B. Hu, X. Zhang, J. Liu, X. Chen, J. Zhao, L. Jin, *Synth. Met.* 228 (2017) 70.
- [11] F.B. Koyuncu, S. Koyuncu, E. Ozdemir, *Org. Electron.* 12 (2011) 1701.
- [12] B. Hu, X. Lv, J. Sun, G. Bian, M. Ouyang, Z. Fu, P. Wang, C. Zhang, *Organ. Electron.* 14 (2013) 1521.
- [13] S. Ertan, A. Cihaner, *Dyes Pigm.* 149 (2018) 437.
- [14] C.-W. Kuo, T.-L. Wu, Y.-C. Lin, J.-K. Chang, H.-R. Chen, T.-Y. Wu, *Polymers* 8 (2016) 368.
- [15] L. Ji, Y.Y. Dai, S.M. Yan, X.J. Lv, C. Su, L.H. Xu, Y.K. Lv, M. Ouyang, Z. Chen, C. Zhang, *Sci. Rep.* 6 (2016) 30068.
- [16] C.-W. Kuo, J.-C. Chang, P.-Y. Lee, T.-Y. Wu, Y.-C. Huang, *Materials* 11 (2018) 1895.
- [17] C.W. Kuo, B.K. Chen, W.B. Li, L.Y. Tseng, T.Y. Wu, C.G. Tseng, H.R. Chen, Y.C. Huang, *J. Chin. Chem. Soc.* 61 (2014) 563.
- [18] N. Atilgan, A. Cihaner, A.M. Önal, *React. Funct. Polym.* 70 (2010) 244.
- [19] T.Y. Wu, J.L. Li, *RSC Adv.* 6 (2016) 15988.
- [20] Y.S. Su, J.C. Chang, T.Y. Wu, *Polymers* 9 (2017) 114.
- [21] T. Soganci, H.C. Soyleyici, M. Ak, H. Cetisli, *J. Electrochem. Soc.* 163 (2016) H59.
- [22] E. Tutuncu, M.I. Ozkut, B. Balci, H. Berk, A. Cihaner, *Eur. Polym. J.* 110 (2019) 233.
- [23] S. Kumar, K.R.J. Thomas, C.-T. Li, K.-C. Ho, *Org. Electron.* 26 (2015) 109.
- [24] D.M. Welsh, A. Kumar, E.W. Meijer, J.R. Reynolds, *Adv. Mater.* 11 (1999) 1379.
- [25] T.Y. Wu, B.K. Chen, L. Hao, K.F. Lin, I.W. Sun, *J. Taiwan Inst. Chem. Eng.* 42 (2011) 914.
- [26] T.Y. Wu, J.W. Liao, C.Y. Chen, *Electrochim. Acta* 150 (2014) 245.
- [27] S.H. Hsiao, H.M. Wang, *RSC Adv.* 6 (2016) 43470.
- [28] T.Y. Wu, H.H. Chung, *Polymers* 8 (2016) 206.
- [29] J. Xu, Q. Ji, L. Kong, H. Du, X. Ju, J. Zhao, *Polymers* 10 (2018) 450.
- [30] S. Mabrouk, M. Zhang, Z. Wang, M. Liang, B. Bahrami, Y. Wu, J. Wu, Q. Qiao, S. Yang, *J. Mater. Chem. A* 6 (2018) 7950.
- [31] T.Y. Wu, R.B. Sheu, Y. Chen, *Macromolecules* 37 (2004) 725.
- [32] S. Tarkuc, M. Ak, E. Onurhan, L. Toppare, *J. Macromol. Sci. Pure Appl. Chem.* 45 (2008) 164.
- [33] K.H. Chang, H.P. Wang, T.Y. Wu, I.W. Sun, *Electrochim. Acta* 119 (2014) 225.
- [34] Z. Bicil, P. Camurlu, B. Yucel, B. Becer, *J. Polym. Res.* 20 (2013) 228.
- [35] N. Guven, P. Camurlu, B. Yucel, *Polym. Int.* 64 (2015) 758.
- [36] M.H. Tsao, T.Y. Wu, H.P. Wang, I.W. Sun, S.G. Su, Y.C. Lin, C.W. Chang, *Mater. Lett.* 65 (2011) 583.
- [37] T.Y. Wu, M.H. Tsao, F.L. Chen, S.G. Su, C.W. Chang, H.P. Wang, Y.C. Lin, W.C. Ou-Yang, I.W. Sun, *Int. J. Mol. Sci.* 11 (2010) 329.
- [38] Y.S. Su, T.Y. Wu, *Polymers* 9 (2017) 284.

- [39] C.-W. Kuo, J.-C. Chang, P.-Y. Lee, T.-Y. Wu, Y.-C. Huang, *Materials* 11 (2018) 1895.
- [40] L. Kong, Z. Wang, J. Zhao, J. Xu, *Int. J. Electrochem. Sci.* 10 (2015) 982.
- [41] T.Y. Wu, Y.S. Su, *J. Electrochem. Soc.* 162 (2015) G103.
- [42] C.W. Kuo, T.Y. Wu, S.C. Fan, *Coatings* 8 (2018) 102.
- [43] G. Xu, J. Zhao, J. Liu, C. Cui, Y. Hou, Y. Kong, *J. Electrochem. Soc.* 160 (2013) G149.

Table 1. Electrochromic images and L^* , a^* , b^* values of homopolymer and copolymer films at various potentials in [EPI⁺][TFSI⁻].

Polymer films	E/V	Photographs	L^* ^a	a^*	b^*
PFPT	0		82.51	1.63	33.23
	1.0		80.68	-1.07	24.1
	1.2		77.66	-1.28	15.7
	1.4		74.24	-0.72	9.29
P(FPT-co-DTC)	0		78.51	-5.31	43.56
	1.0		67.95	-6.53	16.26
	1.2		58.21	-1.13	-2.72
	1.4		56.35	-0.23	-7.15
P(FPT-co-DTP)	0		81.89	15.77	18.07
	0.8		85.48	-0.94	1.99
	1.0		84.46	-1.93	-4.97
	1.2		82.93	-2.4	-7.18

^a L^* represents the lightness, and a^* and b^* denote the color channels.

Table 2. Comparisons of ΔT_{\max} and η_{\max} for several polymer films.

Polymer films	Electrolyte	λ / nm	E_g / eV	ΔT_{\max} / %	ΔOD_{\max} / %	η_{\max} / cm ² C ⁻¹	Ref.
P(TPHA)	0.1 M LiClO ₄ /ACN	334	2.27	11	---	---	32
PSNS-Fc	LiClO ₄ /ACN	356	2.61	27.1	---	---	34
PSNS-iProP	0.1 M TBABF ₄ /ethanol	646	2.28	15.5	7.7	167.4	33
P(SNS-pyrene)	0.1 M LiClO ₄ /ACN	349	3.36	20.28	---	169	35
PFPT	[EPI ⁺][TFSI ⁻]	1320	2.26	22.7	21.1	181.8	This work
P(FPT-co-DTC)	[EPI ⁺][TFSI ⁻]	906	---	44.8	53.4	229.0	This work
P(FPT-co-DTP)	[EPI ⁺][TFSI ⁻]	1212	---	50.7	47.8	232.4	This work

Table 3. Electrochromic images and L^* , a^* , and b^* values of PFPT/PProDOT-Et₂, P(FPT-co-DTC)/PProDOT-Et₂, and P(FPT-co-DTP)/PProDOT-Et₂ ECDs.

ECDs	E/V	Photoimages	L^*	a^*	b^*
PFPT /PProDOT-Et ₂	-0.4		78.4	0.2	17.82
	0.6		64.26	1.02	-8.07
	0.8		58.56	1.63	-16.23
	1.2		55.7	3.59	-20.22
P(FPT-co-DTC)/ PProDOT-Et ₂	-0.4		73.25	-8.16	37
	0.4		57.74	-5.6	13.91
	0.6		50.41	-4.09	3.57
	0.8		43.81	-2.93	-6.28
	1.2		40.63	0.21	-11.51
P(FPT-co-DTP)/ PProDOT-Et ₂	-0.4		73.33	13.82	14.83
	0		75.88	4.55	13.06
	0.4		69.75	-0.49	-4.4
	0.6		64.3	-0.23	-14.5
	0.8		58.63	-1.4	-23.77
	1.2		54.55	4.66	-30.05

Table 4. The transmittance changes and switching time of ECDs.

ECDs	λ/nm	Cycle No.	Optical contrast/%			τ/s		Stability (100 cyc)
			T_b	T_c	ΔT	τ_c	τ_b	
PFPT/PProDOT-Et ₂	590	1	46.1	12.8	33.3	1.01	0.89	99.4%
		50	46.3	13.2	33.1	0.87	0.87	
		100	46.8	13.7	33.1	0.93	0.87	
P(FPT-co-DTC)/PProDOT-Et ₂	586	1	45.3	15.4	29.9	0.86	0.95	98.7%
		50	44.8	15.1	29.7	0.93	0.94	
		100	44.5	15.0	29.5	0.97	0.90	
P(FPT-co-DTP)/PProDOT-Et ₂	612	1	49.4	11.9	37.5	1.03	0.84	98.7%
		50	50.0	11.4	38.6	0.96	0.91	
		100	48.3	11.3	37.0	0.96	0.91	
PDTC/PProDOT-Et ₂ ^a	592	1	---	---	31.3	0.96	0.99	79.5%
		50	---	---	26.8	0.96	0.96	
		100	---	---	24.9	0.99	0.97	
PDTP/PProDOT-Et ₂	591	1	55.7	26.6	29.2	1.05	1.03	97.6%
		50	55.5	26.8	28.7	1.06	1.01	
		100	55.4	26.9	28.5	1.04	1.00	

^a Reference 38.

Table 5. Electrochromic parameters of ECDs.

ECDs	λ/nm	$\Delta T_{\text{max}}/\%$	$\Delta \text{OD}_{\text{max}}/\%$	$\eta/\text{cm}^2\text{C}^{-1}$	Ref.
P(TPHA-co-EDOT)/PEDOT	611	23	---	---	32
PBTC/PEDOT	580	26.3	---	120	40
PBEC/PEDOT	616	20.1	---	399	40
PBDO/PProDOT-Et ₂	586	32.3	37.6	437.5	41
PFPT/PProDOT-Et ₂	590	33.3	53.4	533.5	This study
P(FPT-co-DTC)/PProDOT-Et ₂	586	29.9	47.2	340.0	This study
P(FPT-co-DTP)/PProDOT-Et ₂	612	38.6	61.8	855.9	This study
PDTC/PProDOT-Et ₂	592	31.3	35.6	345.2	38
PDTP/PProDOT-Et ₂	591	29.2	32.2	324.1	This study

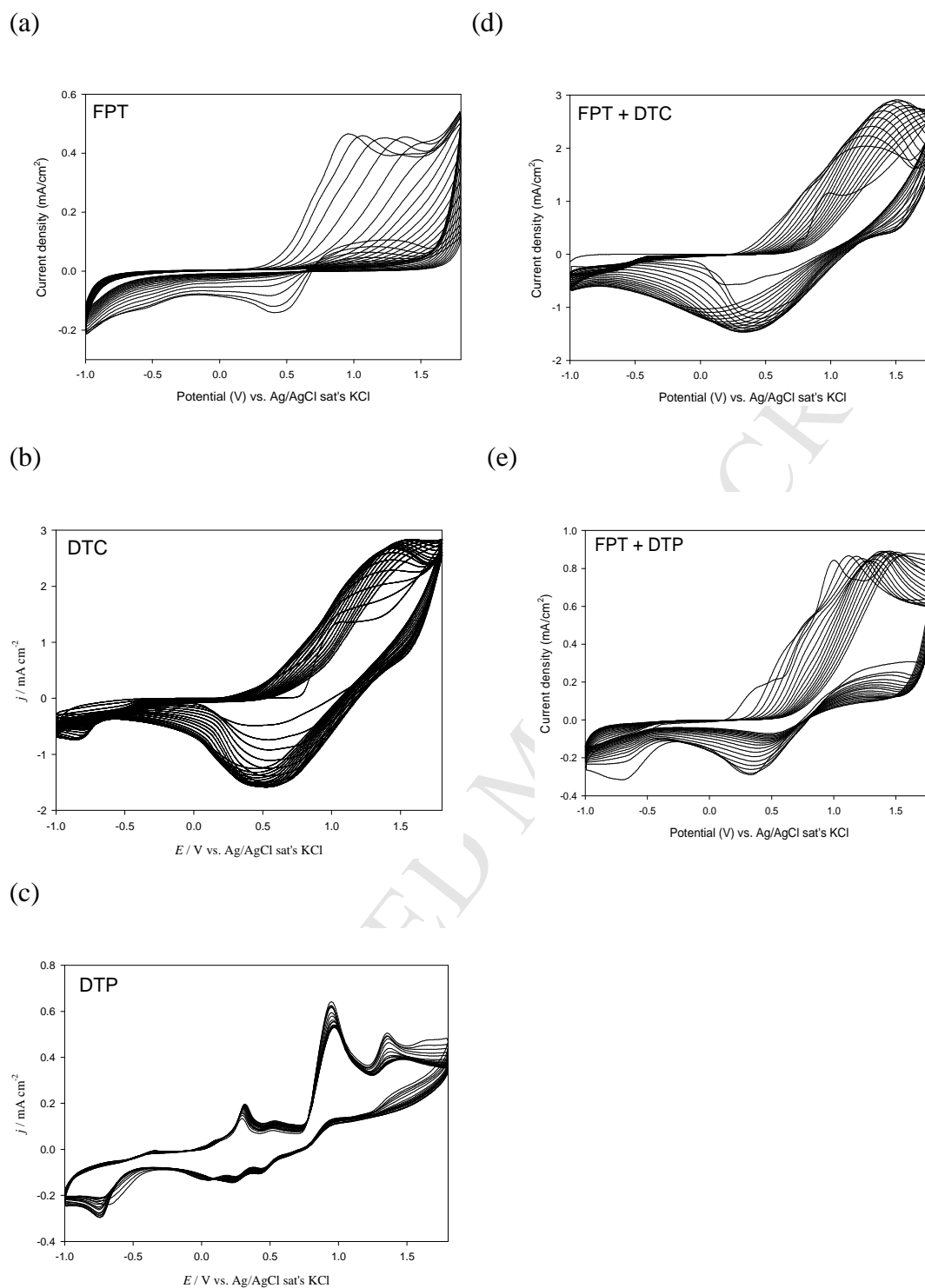


Figure 1. Electrosyntheses of (a) 2 mM FPT, (b) 2 mM DTC, (c) 2 mM DTP, (d) 2 mM FPT + 2 mM DTC, (e) 2 mM FPT + 2 mM DTP in 0.1 M LiClO₄/ACN (scan rate: 100 mV s⁻¹).

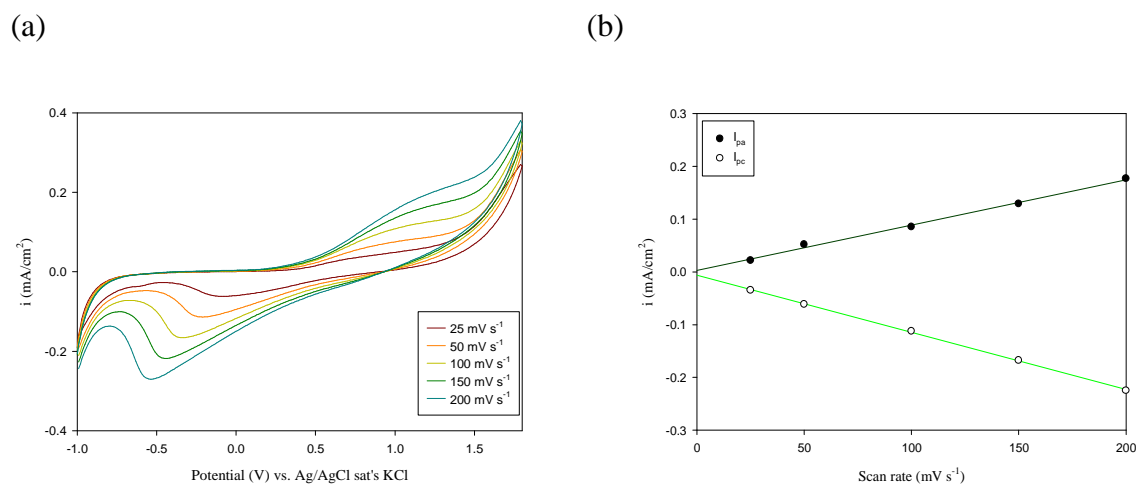
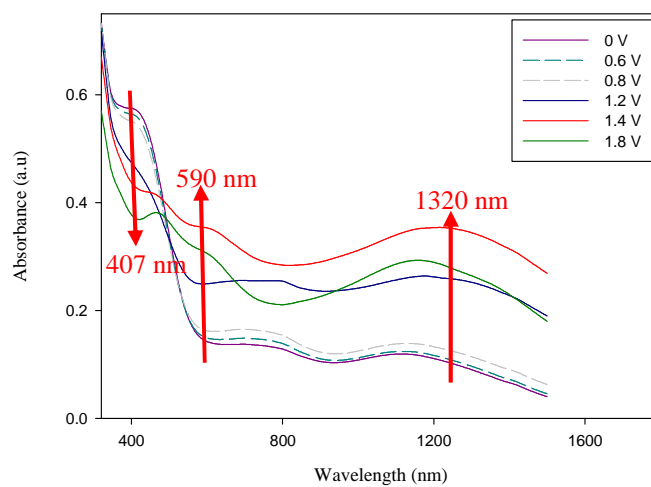
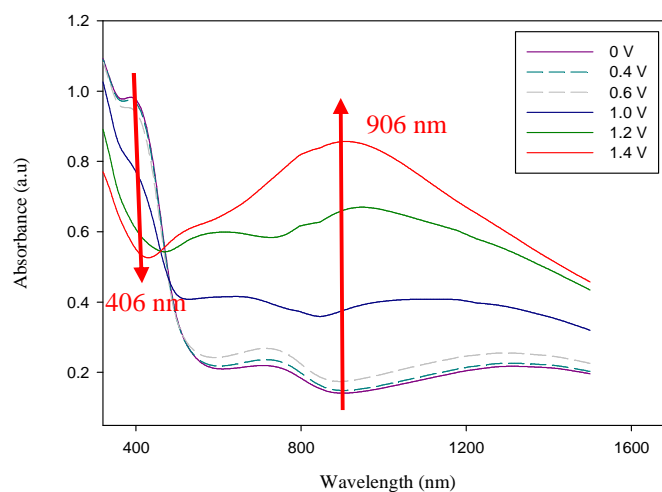


Figure 2. (a) The i - V curves of PFPT film at different scan rates in 0.1 M LiClO₄/ACN; (b) the relationship of scan rates vs. anodic and cathodic peak current densities of PFPT film in 0.1 M LiClO₄/ACN.

(a)



(b)



(c)

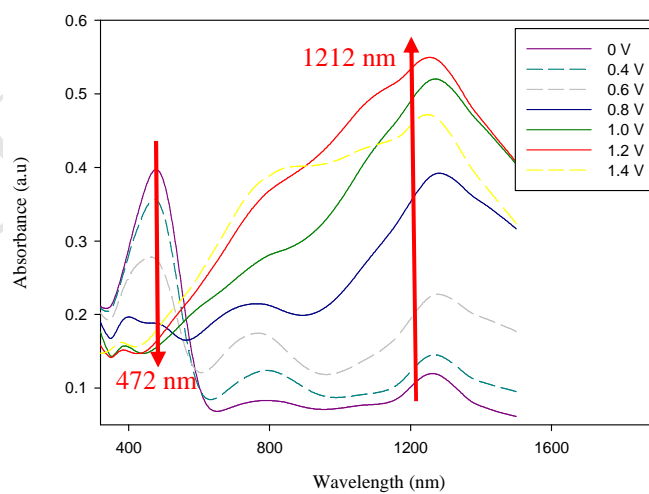
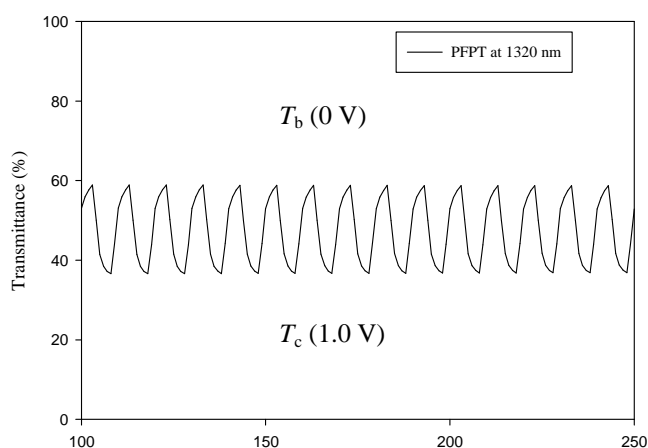
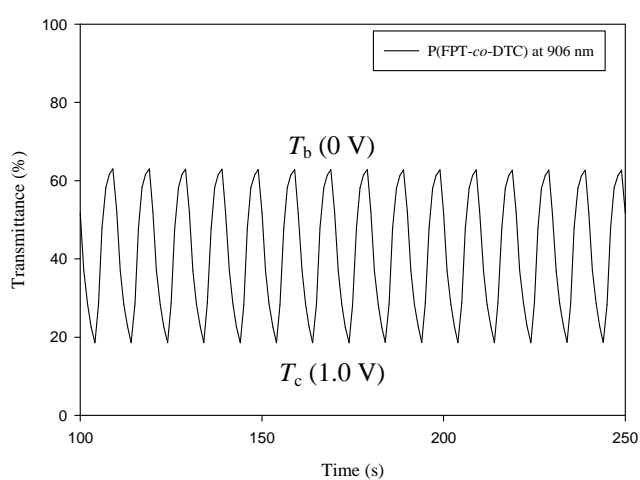


Figure 3. UV-Vis-NIR spectra of (a) PFPT, (b) P(FPT-co-DTC), and (c) P(FPT-co-DTP) films at various potentials in $[EPI^+][TFSI^-]$.

(a)



(b)



(c)

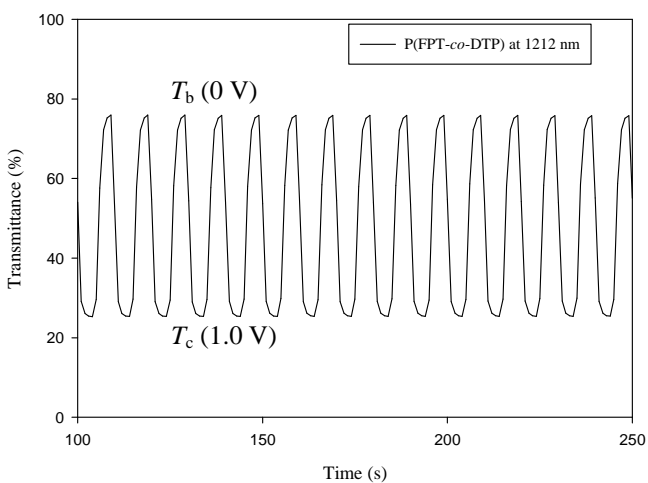


Figure 4. Transmittance-time profiles of (a) PFPT, (b) P(FPT-co-DTC), and (c) P(FPT-co-DTP) films in an ionic liquid with a time interval between bleached and colored states of 5 s.

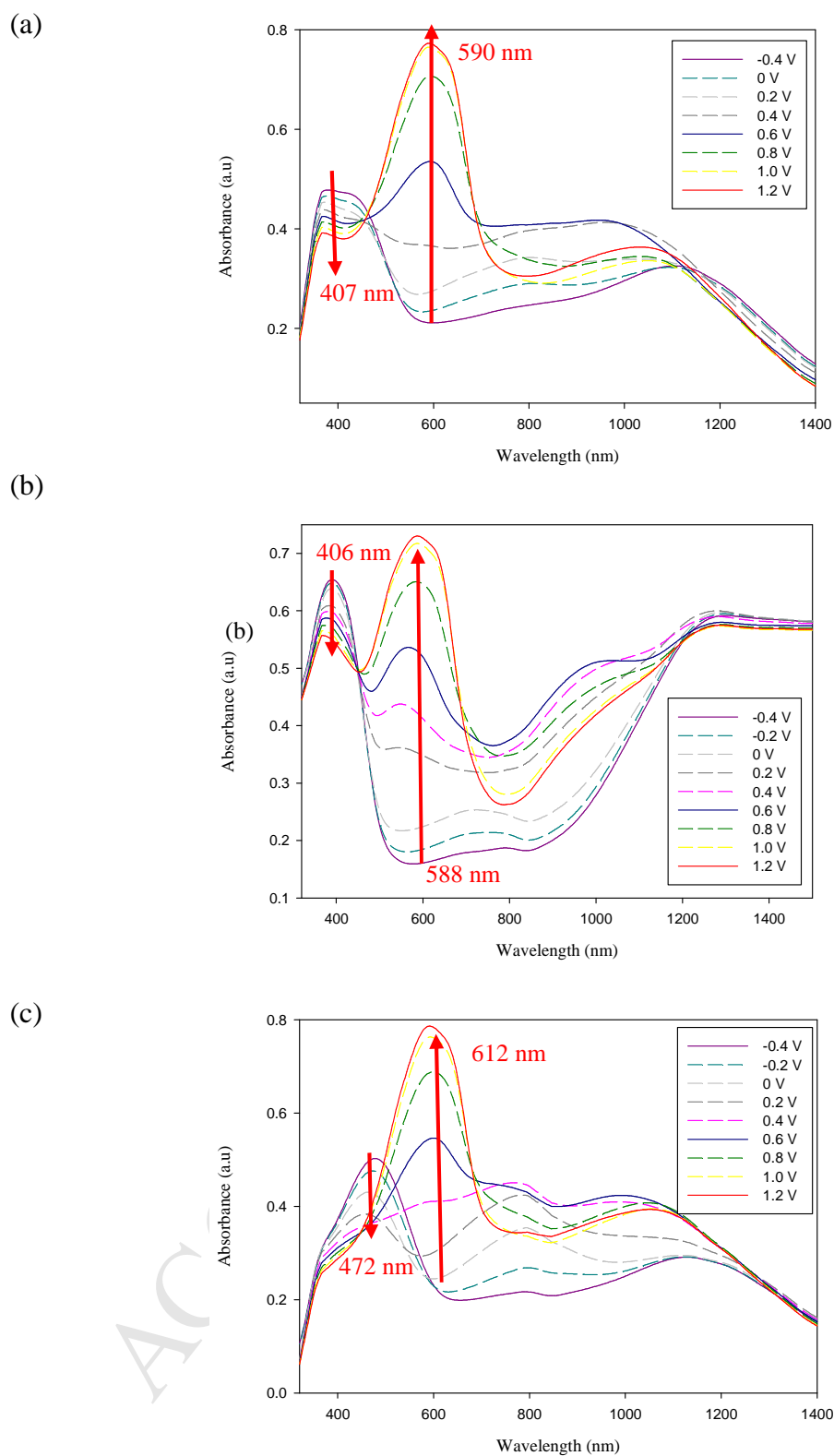
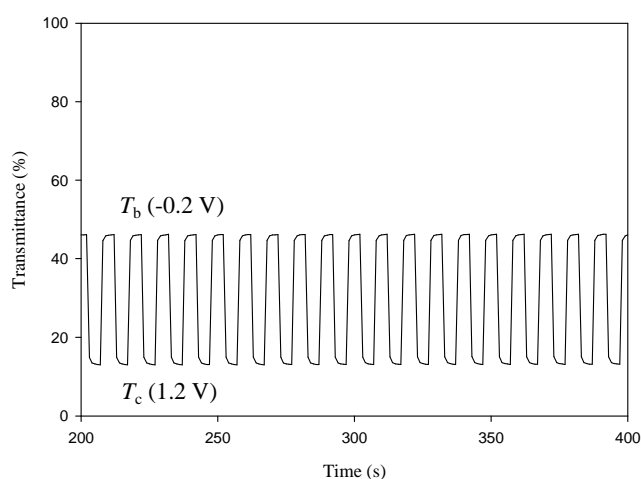
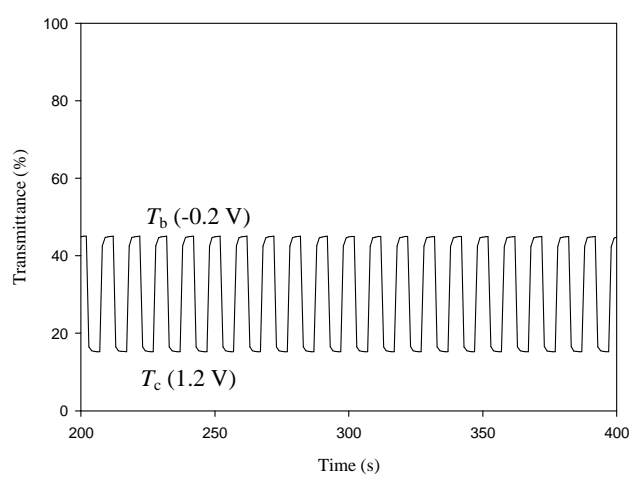


Figure 5. UV-Vis spectra of (a) PFPT/PProDOT-Et₂, (b) P(FPT-co-DTC)/PProDOT-Et₂, and (c) P(FPT-co-DTP)/PProDOT-Et₂ ECDs at different voltages.

(a)



(b)



(c)

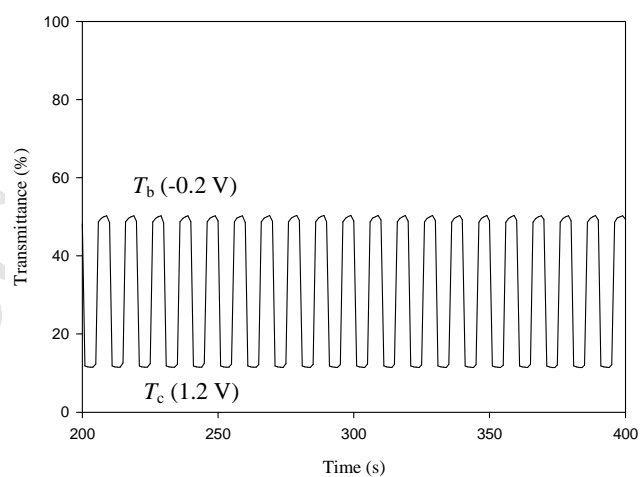
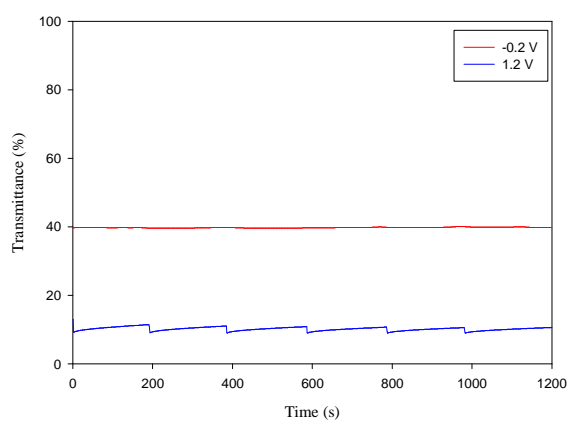
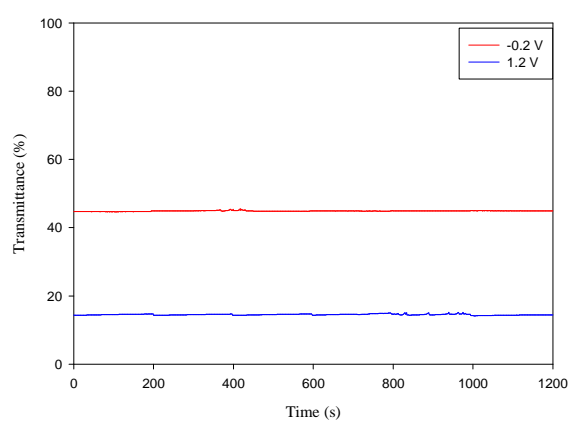


Figure 6. Electrochromic switching of (a) PFPT/PProDOT-Et₂ ECD at 590 nm, (b) P(FPT-co-DTC)/PProDOT-Et₂ ECD at 586 nm, and (c) P(FPT-co-DTP)/PProDOT-Et₂ ECD at 612 nm with a time interval of 5 s. The ECDs were switched between -0.2 V and $+1.2$ V.

(a)



(b)



(c)

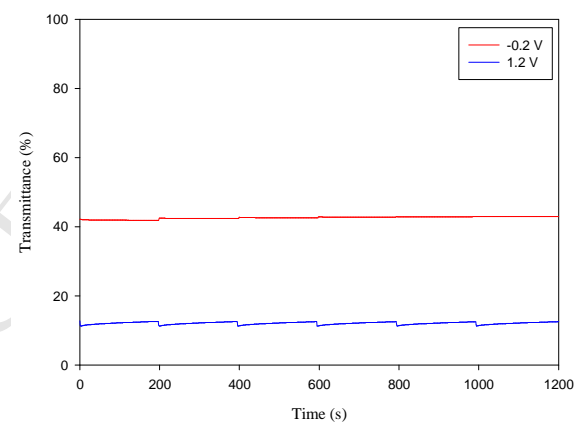
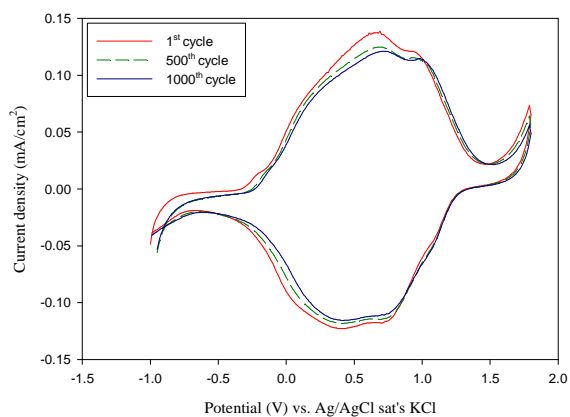
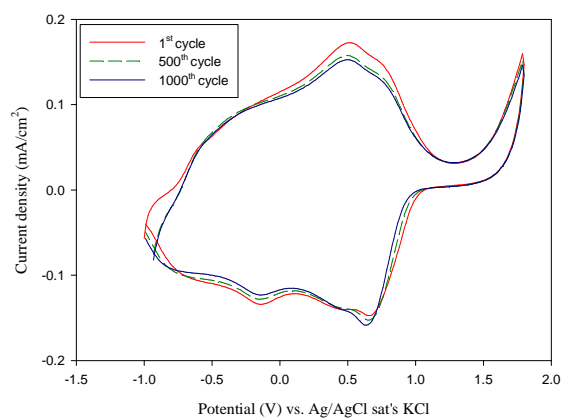


Figure 7. Open circuit memory of (a) PFPT/PProDOT-Et₂ ECD measured at 590 nm, (b) P(FPT-co-DTC)/PProDOT-Et₂ ECD measured at 586 nm, and (c) P(FPT-co-DTP)/PProDOT-Et₂ ECD monitored at 612 nm.

(a)



(b)



(c)

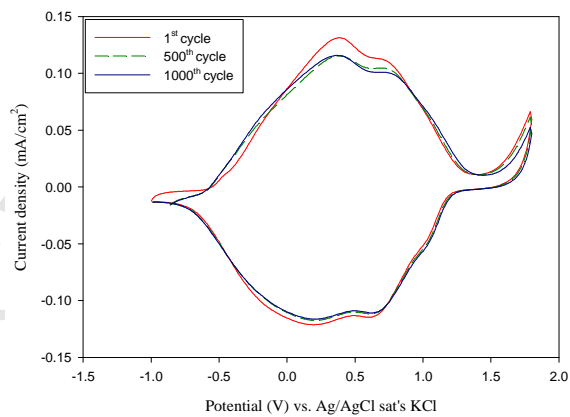
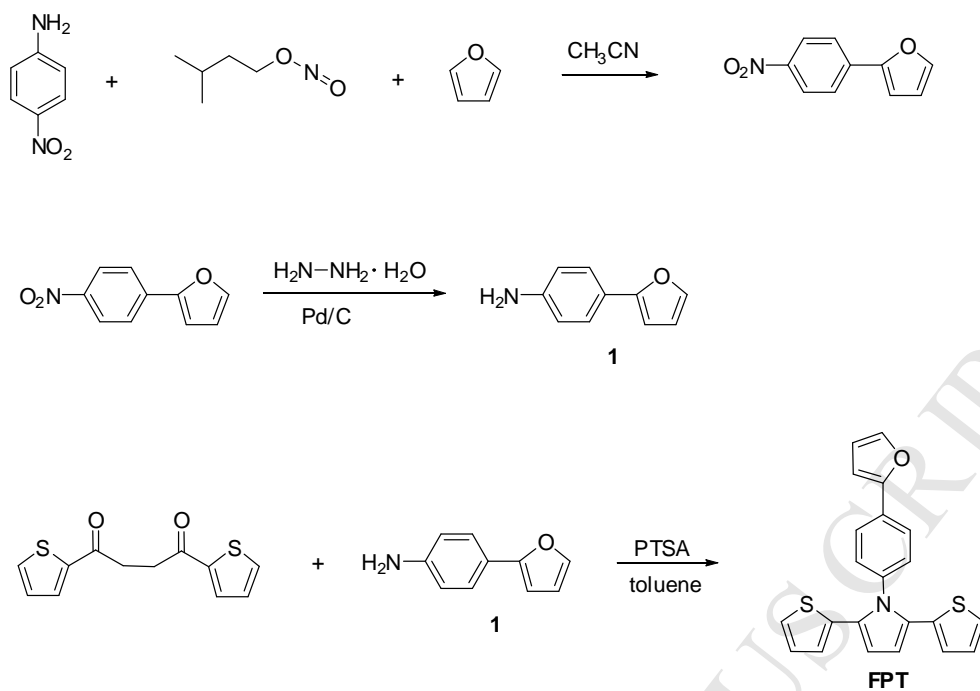
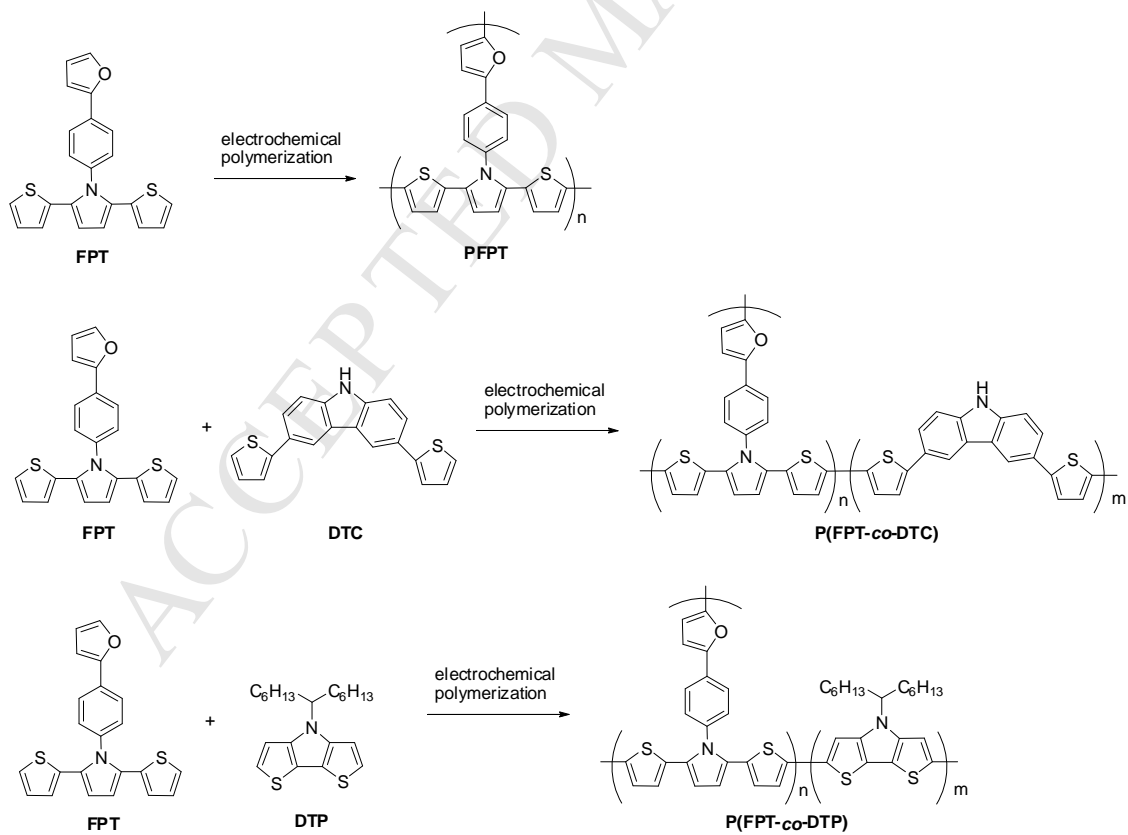


Figure 8. Cyclic voltammograms of (a) PFPT/PProDOT-Et₂, (b) P(FPT-co-DTC)/PProDOT-Et₂, and (c) P(FPT-co-DTP)/PProDOT-Et₂ ECDs at the first, 500th, and 1000th cycles.



Scheme 1. The synthetic procedures of FPT monomer.



Scheme 2. The electrosynthesized schemes of PFPT, P(FPT-co-DTC) and P(FPT-co-DTP).

Highlights

- A 4-(furan-2-yl)phenyl-containing dithienylpyrrole (FPT) was prepared using a Paal-Knorr reaction.
- 4-(furan-2-yl)phenyl-containing polydithienylpyrroles were electrosynthesized.
- P(FPT-*co*-DTP) film displayed conspicuous color variations ranging from brass, gray, grayish-blue to blue.
- PFPT/PProDOT-Et₂ ECD realized high ΔT_{\max} (33.3%) and η (533.5 cm² C⁻¹).
- ECDs showed long-term reversible redox behaviors.